

Magnetic resonance diffusion tensor imaging and diffusion tensor tractography of human visual pathway

Yan Zhang¹, Si-Hai Wan², Gui-Jun Wu³, Xue-Lin Zhang^{2,4}

Foundation item: Fundamental Research Funds of State Key Laboratory of Ophthalmology, China

¹ Zhongshan Ophthalmic Center, State Key Laboratory of Ophthalmology, Sun Yat-sen University, Guangzhou 510060, Guangdong Province, China

²Department of Radiology, Nanfang Hospital, Southern Medical University, Guangzhou 510515, Guangdong Province, China

³Department of Ophthalmology, Nanfang Hospital, Southern Medical University, Guangzhou 510515, Guangdong Province, China

⁴ Department of Radiology, Kanghua Hospital, Dongguan 523080, Guangdong Province, China

Correspondence to: Xue-Lin Zhang. Department of Radiology, Nanfang Hospital, Southern Medical University, Guangzhou 510515, Guangdong Province, China. zxlxfy@163.com

Received: 2012-01-08

Accepted: 2012-06-20

Abstract

• **AIM:** To investigate the visual pathway in normal subjects and patients with lesion involved by diffusion tensor imaging (DTI) and diffusion tensor tractography (DTT).

• **METHODS:** Thirty normal volunteers, 3 subjects with orbital tumors involved the optic nerve (ON) and 33 subjects with occipital lobe tumors involved the optic radiation (OR) (10 gliomas, 6 meningiomas and 17 cerebral metastases) undertook routine cranium magnetic resonance imaging (MRI), DTI and DTT. Visual pathway fibers were analyzed by DTI and DTT images. Test fractional anisotropy (FA) and mean diffusivity (MD) values in different part of the visual pathway.

• **RESULTS:** The whole visual pathway but optic chiasm manifested as hyperintensity in FA maps and homogenous green signal in the direction encoded color maps. The optic chiasm did not display clearly. There was no significant difference between the bilateral FA values and MD values of normal visual pathway but optic chiasm, which the FA values tested were much too low (all $P > 0.05$). The ONs of subjects with orbital tumors were compressed and displaced. Only one

subject had lower FA values and higher MD values. OR of 9 gliomas subjects were infiltrated, with displacement in 2 and disruption in 7 subjects. All OR in 6 meningiomas subjects were displaced. OR in 17 cerebral metastases subjects all developed displacement while 7 of them had disruption also.

• **CONCLUSION:** MR-DTI is highly sensitive in manifesting visual pathway. Visual pathway can be analyzed quantitatively in FA and MD values. DTT supplies accurate three dimensional conformations of visual pathway. But optic chiasm's manifestation still needs to improve.

• **KEYWORDS:** visual pathway; human; diffusion tensor imaging; diffusion tensor tractography

DOI:10.3980/j.issn.2222-3959.2012.04.09

Zhang Y, Wan SH, Wu GJ, Zhang XL. Magnetic resonance diffusion tensor imaging and diffusion tensor tractography of human visual pathway. *Int J Ophthalmol* 2012;5(4):452-458

INTRODUCTION

The visual pathway originates from the retinal photoreceptors. The axons of retinal ganglion cells gather together and form the optic nerve. The optic nerve extends and forms the optic tract after the optic chiasm. The lateral geniculate nucleus (LGN) acts as a relay nucleus of the optic tract. The optic radiation, which originates from the LGN and comprises primarily fibers of the optic tract, is shaped like a convex lamina. It extends into the lateral sagittal plane beside the paracale and projects to the visual center in the occipital lobe^[1-2]. The visual pathway is a white matter (WM) bundle composed of medullated fibers. It conducts nervous impulses transformed from optical visual information to the visual center in the occipital lobe (Figure 1,2).

The principle of magnetic resonance imaging (MRI) is to apply a radiofrequency pulse to the human body, which is placed inside a magnetic field. The hydrogen atoms of the human body produce signals, which software then converts to images. Diffusion tensor imaging (DTI) images the random-walk motion of water molecules using appropriate defocusing and refocusing gradients, although the principle

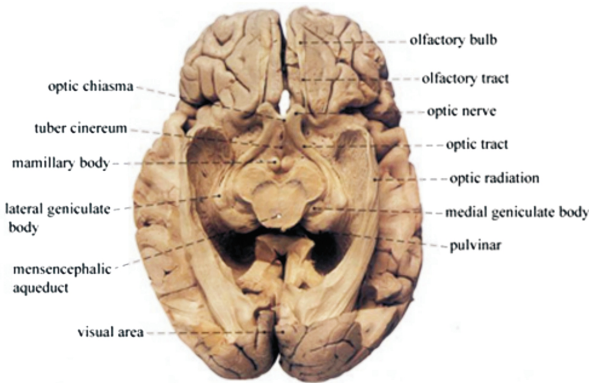


Figure 1 Optic pathway in a brain dissection.

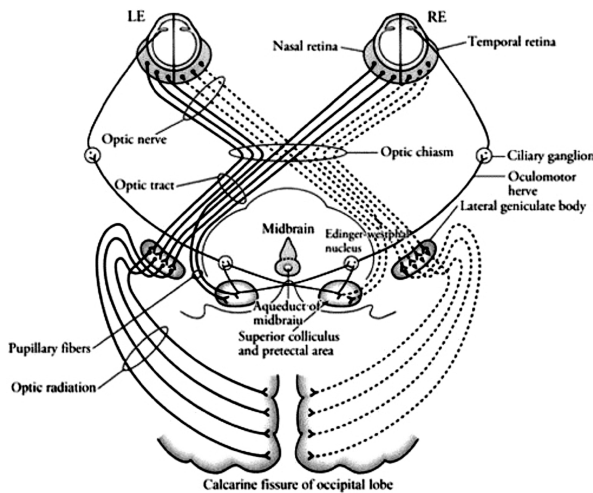


Figure 2 Schematic diagram of optic pathway.

of image acquisition and formation are the same as conventional MRI. Thus, DTI is a technique used to measure the speed of drifting water molecules per unit time. It then uses those data to build images^[3]. The parameters of DTI are called diffusion indices. Diffusion indices included the FA and MD. The FA value reflects the direction of and the MD value reflects the speed of diffusion, mainly^[4-6]. These values can be expressed either as a number or as a directionally encoded colour map. A change in these indices provides information on underlying microanatomic changes or pathological changes of WM fiber bundles^[1,2,7,8]. Diffusion tensor tractography (DTT) is a computational procedure that reconstructs major fiber bundles in three-dimensional spaces based on their anisotropy properties. It is the most visual method for presenting target tracts from DTI data. DTI is the only available non-invasive imaging techniques to display and quantitatively analyze white matter nerve fibers *in vivo*^[9]. It has been used to evaluate corticospinal tracts and got satisfied results^[10]. We depicted the visual pathway with DTI and conformed the tractography of nerve fibers clearly. This may be helpful to diagnosis and therapy diseases with visual pathway involved.

SUBJECTS AND METHODS

Subjects Thirty healthy volunteers (15 men and 15 women, age of 20-60 years, mean age 40.34 years), none of

which had orbit disease, neurological disease or vision abnormality. There was no symptom and positive finding in physical exam of nervous system. No abnormality in routine cranium MRI and diffusion weighted imaging (DWI). Three patients (1 man and 2 women, age of 48, 53 and 49 years) had orbital tumors that involved the optic nerve, including 1 meningioma and 2 cavernous hemangiomas. Thirty-three patients (18 men and 15 women; age of 35-77 years; mean age of 52.2 years) had occipital lobe tumors that involved the optic radiation (OR). There were 10 gliomas, with 9 astrocytomas (WHO grade II, 7 cases; grade III and IV, 2 cases) and 1 ependymoma; 6 meningiomas, and 17 metastatic tumors (lung cancer, 7 cases; breast cancer, 2 cases; gastric cancer, 1 case). All cases were certified by pathology specimens and clinical evidences.

Methods

MRI MRIs were performed using a 1.5-Tesla scanner (Sigma Twin, GE, USA) with an 8-channel head-phased array coil. Magnetic-field gradients permit up to 40mT/m/s amplitude and a magnetic-field-gradient switching rate of up to 120mT/m/s. All the subjects took routine cranium MRI, which included T₁WI, T₂WI, and FLAIR sequence. In T₁WI-FLAIR, TR/TI/TE 2500/750/11.9ms, slice thickness 5mm, inter-slice separation 1.5mm, matrix size=320mm×256mm, FOV 240mm×180mm, double collections. In T₂WI, TR/TE 4900/99.3ms, slice thickness 5mm, inter-slice separation 1.5mm, matrix size= 320mm×224mm, FOV 240mm×180mm, double collections. In T₂WI-FLAIR, TR/TE 8500/128ms, slice thickness 5mm, inter-slice separation 1.5mm, matrix size =320mm×192mm, FOV 240mm×240mm, single collection.

DTI was performed in the axial plane using a spin echo-echo planar imaging (SE-EPI) diffusion tensor sequence after routine MRI scanning (repetition time (TR) = 6000ms; echo time (TE) = 60.1ms; field of view (FOV) 240mm×240mm; b=1000s/mm²; 2 NEX; diffusion-sensitive gradient direction with 13; matrix size = 128mm×128mm; 3.5mm slice thickness; inter-slice separation 0).

Date and image process Process primary data with software Volume One 1.72 (GE Corp., USA) and diffusion Tensor Visualizer 1.72 (Tokyo University, Japan) and get directionally encoded color (DEC) maps, which include the color fractional anisotropy (FA) map and the black-white FA map. Fibers of different directions are demonstrated as different colors, red color as the x element(left-right), green color as the y element (anterior-posterior) and blue color as the z element (superior-inferior).

The region of interest (ROI) were as follows: The orbital part of the optic nerve (in green color) in recombined coronal plane DEC maps was selected. The surrounding part of the cerebral peduncle in recombined coronal plane DEC maps was selected as the ROI of the optic tract. The

Table 1 FA and MD values ($\text{is} \times 10^{-3} \text{mm}^2/\text{s}$) of visual pathway in normal subjects ($\bar{x} \pm s$)

Location	Optic nerve		Optic tract		Optic radiation	
	Left	Right	Left	Right	Left	Right
FA	0.595±0.067	0.589±0.066	0.531±0.062	0.526±0.052	0.509±0.029	0.502±0.026
MD	0.948±0.112	0.932±0.088	0.944±0.131	0.935±0.113	0.763±0.050	0.748±0.052
<i>t</i>	0.497	¹ 0.844	0.468	¹ 0.380	1.761	¹ 1.792
<i>P</i>	0.623	¹ 0.406	0.643	¹ 0.707	0.089	¹ 0.084

¹the value in MD comparison.

anterior-posterior optic radiation (in green color) beside the ventricle triangle in axial plane DEC maps was selected as the ROI of the optic radiation. Measure the anterior, moderate and posterior point of the ROI to get the mean value in the optic nerve and the optic tract. Measure three continuous planes and obtain the mean value in the ROI of the optic radiation.

We used line propagation techniques in this research. Primary DTI data of 10 volunteers were processed with the post-processing software, the diffusion TENSOR Visualizer (dTV) 1.72 (Laboratory of imaging analyzing, institute of radiology, affiliated hospital of university of Tokyo). The seed points were set with manual selection in bilateral optic nerve, chiasm, and optic tract in the chiasm section of DEC map, which expressing X shape. The termination conditions were $FA < 0.20$, $step < 160$, $So < 160$. The LGN which locates at the posterior lateral of the thalamus in cross section was set as the seed point and occipital lobe as the termination region in the DEC map or DWI map. The termination conditions were $FA < 0.18$, $step < 160$, $So < 160$.

Demographic informations on MRI scans were masked and the patients were presented randomly and in a blinded fashion to three neuroradiologist for determination of abnormalities. Reproducibility was assessed by presenting five of the scans a second time to the same neuroradiologists.

Statistical Analysis The results of patients were analyzed using independent-sample *T*-tests in the SPSS11.0 software (IBM SPSS Corp., USA). The results of healthy subjects were analyzed using paired *T* test. $P < 0.05$ was considered statistically significant. This study was approved by the local Human Research Protection Office/ Institutional Review Board an all subjects provided written informed consent. The study followed the Declaration of Helsinki.

RESULTS

All the 30 volunteers completed this research. On the DEC maps, 24 cases were clear while 6 cases had slight serrated artifacts at the rim of optic nerves. The optic nerves manifested as hyperintensity in FA maps. In the DEC maps, they were green and clear. Their signal intensity was almost the same as the rectus. The optic chiasm did not displayed clearly in the FA maps and the FA values tested were much

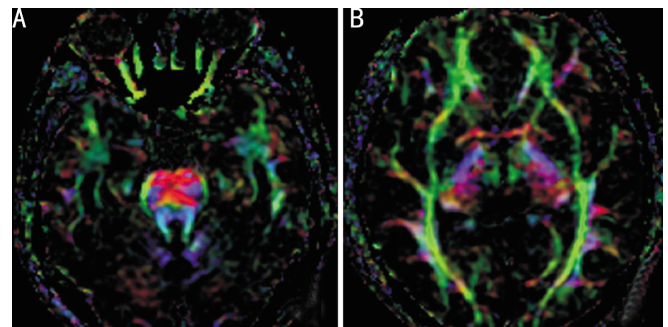


Figure 3 DEC maps of visual pathway A: Optic nerve; B: Optic radiation.

too low. The optic chiasm could not be shown clearly after reconstruction of the images in sagittal and coronal view (Figure 3A). The optic tract was displayed clearly in the DTI maps. It manifested as hyperintensity in FA maps. In DEC maps, it always manifested as red or green according to the angle of it and the central sagittal view. Optic radiation was fan-shaped, processed through the temporal lobe, parietal lobe and occipital lobe and terminated at the visual cortex in occipital lobe. It manifested as high signal in the FA maps. In DEC map the optic radiation was manifested as homogenous green high signal. It was smooth and natural, which could be distinguished easily with other fibers^[8] (Figure 3B).

The FA value and the MD value of normal visual pathway were displayed in the Table 1. There was no significant difference between the bilateral FA values and MD values of optic nerve, optic tract and optic radiation (all $P > 0.05$).

The anterior visual pathway could be manifested well in FA map, DEC map and DTT map (Figure 4A, B). Meanwhile, the DTT map displayed the small quantity optic radiation bundles from optic tract *via* LGN backwards, which provided a clear anatomic location for taking LGN as the seed point of tracking optic radiation fiber bundles (Figure 4C). Optic radiations were fan shaped, originated from LGN, *via* temporal lobe, parietal lobe and occipital lobe and terminated at visual cortex of occipital lobe (Brodmann 17 area) (Figure 4B).

The ONs of orbital tumors subjects were compressed and displaced. Only one subject had lower FA values and higher MD values in ON (FA=0.24, MD= $1.75 \times 10^{-3} \text{mm}^2/\text{s}$) (Figure 5).

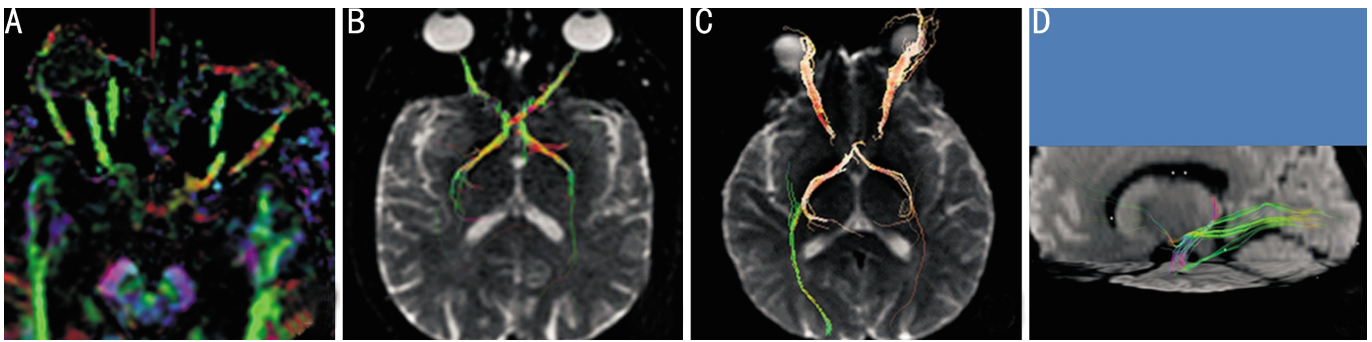


Figure 4 Nerve fiber conformation images of the visual pathway A: Bilateral optic nerves; B: Fiber tractography conformation image of the anterior visual pathway; C: Fiber conformation image of right optic radiation; D: DTT map of optic radiation after reconstruction.

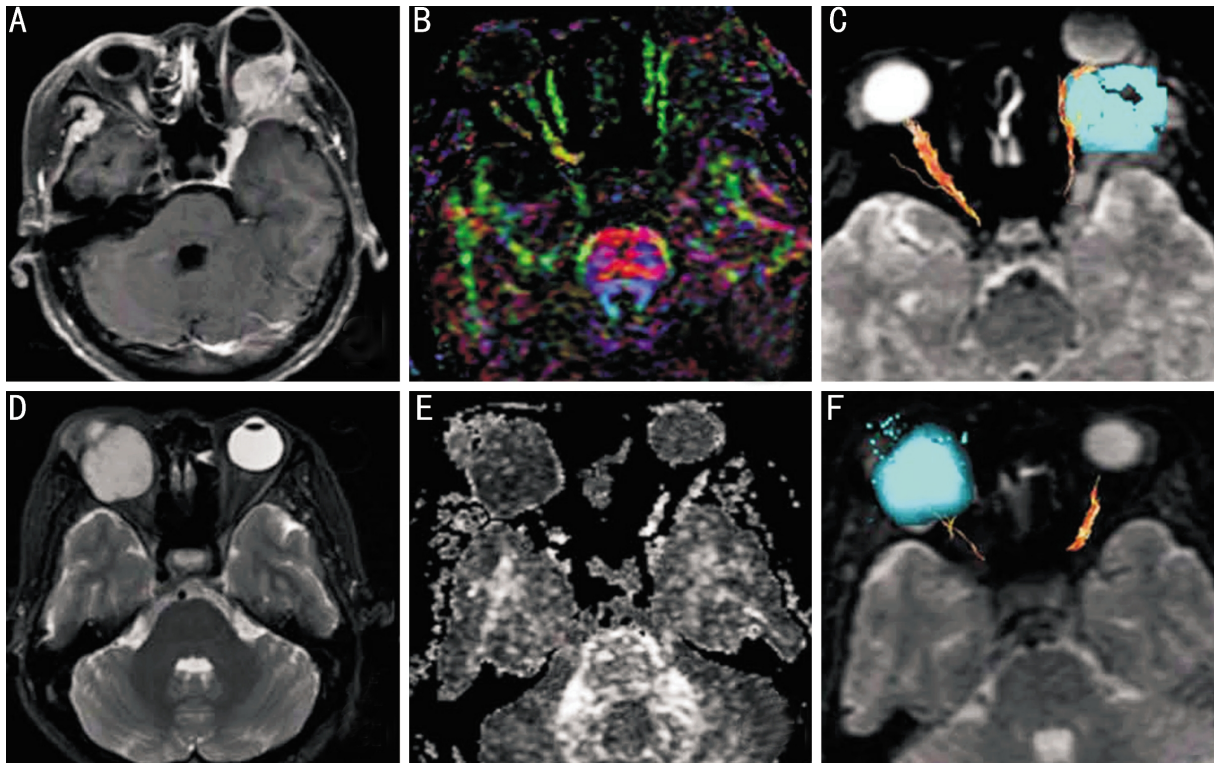


Figure 5 Left orbital invasive meningioma in a 53 years old woman The mass is enhanced on contrast T₁WI image (A). The left optic nerve is compressed and displaced with normal FA value on DEC image(B) and DTT image(C). Right orbital angiocavernoma in a 49 years old woman. The mass is hyperintensity on fat saturated T₂WI image(D). The right optic nerve is compressed and displaced with reduced FA values on FA image (E). In DTT image (F), the right optic nerve is displaced and atrophied significantly compared with contralateral optic nerve (red).

Ciccarelli *et al*^[11] categorized the WM tracts as edematous, displaced, disrupted or infiltrated with neoplasms: 1) displaced, the WM tracts had abnormal pattern and location but normal fractional anisotropy; 2) disrupted, the WM tracts disappeared in FA images with significant fractional anisotropy decrease; 3) infiltrated, the WM tracts had abnormal pattern and location. Its fractional anisotropy decreased. But in FA images, the tracts still can be identified.

The OR in glioma group were mostly infiltrated. The tracts only had displacement in astrocytomas grade II since it was a tumor of low invasion. OR in astrocytomas grade III and IV were disrupted (Figure 6). The OR in ependymoma was disrupted and displaced (Figure 7). The OR in meningiomas

were compressed and shifted and appeared like a cup but with no fracture or interruption (Figure 8). DTT images showed that OR in metastases all had displacement while most accompanied with disruption (Figure 9).

DISCUSSION

Visual pathway originates from the retina and terminates in the visual cortex of occipital lobe. It includes the optic nerves, optic chiasm, optic tract, LGN, optic radiation and visual cortex of occipital lobe. Though the visual pathway has several grades of neurons, the white matter fibers contained the most part of visual pathway.

The diffusion tensor imaging of optic nerve may generate artifacts easily because the effect of surrounding fat, cerebrospinal fluid, air in sinonasals and ocular movement.

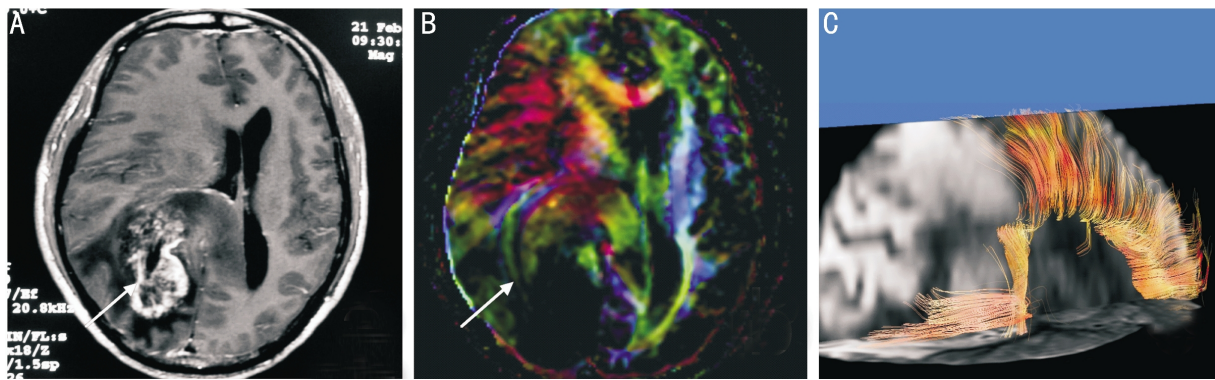


Figure 6 Right occipital lobe glioblastoma in a 55 years old man A: The mass (arrow) is marked enhancement on contrast T_1 WI; B: The FA value of the right optic radiation decreases and it cannot be identified in DEC map; C: DTT map shows disruption and infiltration of right optic radiation (red).

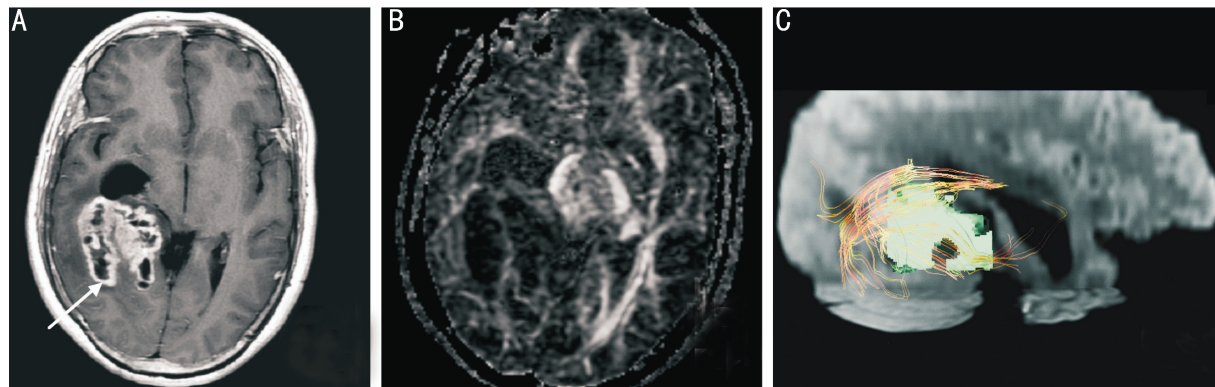


Figure 7 Right trigone of lateral cerebral ventricle endypnoma in a 33-year-old man A: The mass (arrow) is marked enhancement on contrast T_1 WI map; B: The FA value of right optic radiation decreases in FA map; C: DTT map shows disruption and displacement of optic radiation (red).

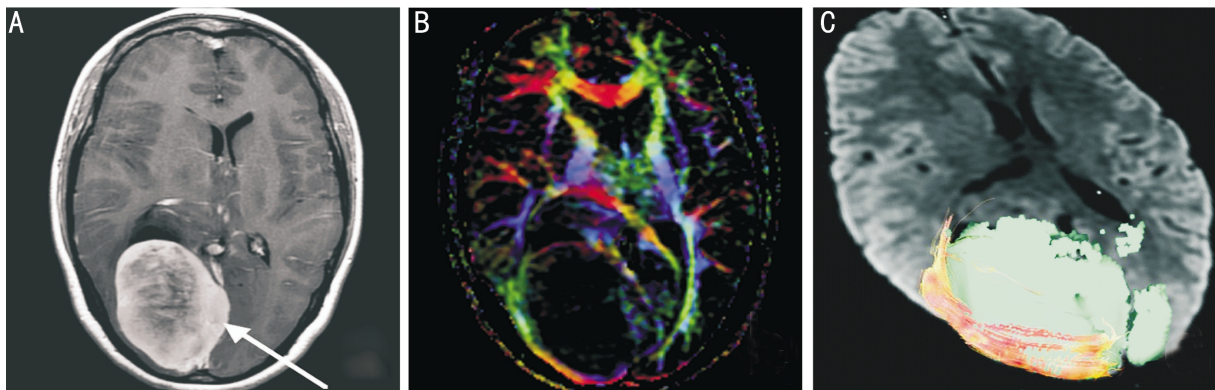


Figure 8 Meningioma of right occipital lobe in 42 years old woman A: The mass (arrow) is marked enhancement on axial contrast T_1 WI map; B: The FA value of right optic radiation decreases in DEC map; C: DTT map shows the displaced right optic radiation (red) and tumor (blue).

This limits the application of DTI. With the development of MRI in recent year ^[9], Wheeler-Kingshott *et al* ^[12] reported the zonal oblique multislice echoplanar imaging (ZOOM-EPI) inhibited fat and cerebrospinal fluid simultaneously. This imaging technique can inhibit the high signal of fat and cerebrospinal fluid surrounding optic nerve effectively and gain the FA value and MD value of optic nerve, which makes the application of MR-DTI in clinic become possible.

The moving speeds of water molecules in nervous fibers relate to the direction of the fibers^[9,12]. When the direction of

the moving water molecules is coincident with that of the fibers, the water molecules will experience minimal limitation and thus exhibit maximal speed. When their direction is perpendicular to that of the fibers, the water molecules will experience maximal limitation and thus exhibit minimal speed. Thus, the character of water molecules can divulge important information on the direction of the visual pathway fibers ^[13]. DTT is a computational procedure that reconstructs major fiber bundles in three-dimensional spaces based on their anisotropy properties ^[14]. It is the most visual method for

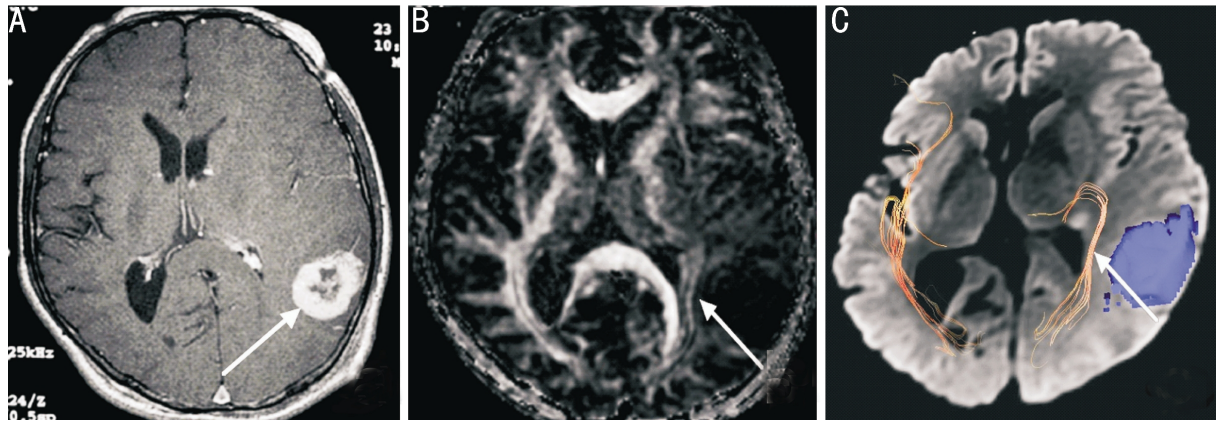


Figure 9 Metastatic tumor of right occipital lobe in a 71-year-old man with lung cancer A: The mass (arrow) is marked enhancement on contrast T₁WI map; B: The FA value of left optic radiation decreases in DEC map; C: DTT map shows the left fiber tract is disrupted by the tumor (blue).

presenting target tracts from DTI data. Function damage and possible outcome can be estimated from stereoscopic images of target WM tracts.

In this research, we analyzed the nerve fibers of visual pathway quantitatively. The FA value and MD value of bilateral optic nerve, optic tract and optic radiation were measured in 30 healthy adult volunteers. The result showed: 1) There was no significant difference between the FA value and MD value in bilateral optic nerve, optic tract and optic radiation; 2) The fractional anisotropy value of nerve fibers in different parts of visual pathway had a little differences. The FA value of optic nerve was the highest, followed by the optic tract and optic radiation. The reason might be that the fibers of optic nerve and optic tract were intensive while the optic radiation relatively dispersed.

Neither FA map nor DEC map display optic chiasm clearly. It is mainly because the decussating fibers in optic chiasm weak the single direction dominant of hydrone dispersion. Displaying of optic chiasm may need to be further studied^[15]. DTI is highly sensitive to the nerve fibers of visual pathway and displays the abnormal signal change of visual pathway clearly. FA values and MD values can quantitatively evaluate optic nerve fibers' demyelination, axonal degeneration and disintegration^[16].

Routine MR sequences can evaluate the location of intracranial neoplasm. But the location relationship of neoplasm and WM tracts nearby, the integrity of WM tracts and its infiltration by tumor tissues are not definite. DTI can noninvasively evaluate the WM integrity and fiber connectivity *in vivo*, yet the connections of adjacent voxels are unavailable^[17].

The FA values of disrupted WM tracts decrease significantly. Consequently, the tracts disappear in FA images, which represent the FA values. The FA value reflects the directionality of water diffusion in each voxel, the decrease of it suggests the diffusion has lost the main

directionality. Since the path of a water molecule along a white matter fiber is constrained by physical boundaries such as the axon sheath, diffusion along the long axis of a fiber (axial or longitudinal diffusion) is greater than diffusion across the fiber (radial or transverse diffusion)^[17-19]. This suggests an alteration in axonal density and axonal arrangement. OR disruptions always develop in high grade astrocytomas (grade III and IV), ependymoma and metastases. The vision recovery is pessimistic.

The infiltration of WM tracts is a deformation between displacement and disruption. The WM tracts have abnormal pattern and location. Their FA values decrease. But they still can be identified in FA images. This suggests the axon destructions in infiltration are less than in disruption. OR infiltrations all develop in astrocytomas in our study. The reason may be astrocytomas originate from normal nervous tissue, the gliocyte. The OR is gradually destroyed by tumor cells with the malignant grades of astrocytomas increases.

Orbital tumor impresses the optic nerve and causes visual fields change is quite common in ophthalmological clinic. However, it is not clear whether impressed nerve is degenerated or necrotic. Now we can make judgment with MR-DTI whether the degeneration is reversible or not after years. The smaller the FA value is, the bigger possibility of necrosis, vice versa. This is because hydrones lose the direction dominant after tissue necrosis, and the anisotropy decreases and the FA value decreases, as a result, the isotropy and the MD value also increases^[3,18].

DTI-derived measures are valid markers of OR impairment in intracranial neoplasms. OR change varies according to the properties of lesions.

With the development of a dvanced imaging tools, DTI makes a significant impact in the clinical imaging of patients with neurological diseases involved OR. Yielding structural and functional information about ordered WM pathways in

the brain, DTI can assist neurosurgeons in identifying conditions occult to structural imaging and provide relational information that is critical to neurosurgery decision making^[19]. It can help ophthalmologists to predict the destruction of optic tracts and vision prognosis^[20,21].

REFERENCES

- 1 Miller NR. Diffusion tensor imaging of the visual sensory pathway: are we there yet? *Am J Ophthalmol*2005; 140(5): 896–897
- 2 Wan SH, Zhang XL, Sun X, Xiao XL, Xing HF. The initial clinical application of MR DTI and DTT in the adult optic radiation. *Linchuang Fangshexue Zazhi*2007;26(11): 1076–1079
- 3 Basser PJ, Pajevic S, Pierpaoli C, Duda J, Aldroubi A. *In vivo* fiber tractography using DT-MRI data. *Magn Reson Med*2000;44(4):625–632
- 4 LeBihan D, Mangin JF, Poupon C, Clark CA, Pappata S, Molkon N, Chabriat H. Diffusion tensor imaging: concepts and applications. *J Magn Reson Imaging*2001;13(4): 533–546
- 5 Mamata H, Mamata Y, Westin CF, Shenton ME, Kikinis R, Jolesz FA, Maier SE. High-resolution line scan diffusion tensor MR imaging of white matter fiber tract anatomy. *AJNR*2002;23(1):67–75
- 6 Mori S, vanZijl PC. Fiber tracking: principles and strategies—a technical review. *NMR Biomed*2002; 15(7): 468–480
- 7 Chanraud S, Zahr N, Sullivan EV, Pfefferbaum. A MR diffusion tensor imaging: a window into white matter integrity of the working brain. *Neuropsychol Rev*2010;20(2):209–225
- 8 Parekn MB, Carney PR, Sepulveda H, Norman W, King M, Mareci TH. Early MR diffusion and relaxation changes in the parahippocampal gyrus precede the onset of spontaneous seizures in an animal model of chronic limbic epilepsy. *Exp Neuro*2010;224(1):258–270
- 9 Bammer R, Acar B, Moseley ME. *In vivo* MR tractography using diffusion imaging. *Eur J Radiol*2003;45(3): 223–234
- 10 Mukherjee P. Diffusion tensor imaging and fiber tractography in acute stroke. *Neuroimaging Clin N Am*2005;15(3):655–665
- 11 Ciccarelli O, Toosy AT, Parker GJ, Wheeler-Kingshott CA, Barker GJ, Miller DH, Thompson AJ. Diffusion tractography based group mapping of major white-matter pathways in the human brain. *Neuroimage*2003;19(4):

- 1545–1555
- 12 Wheeler-Kingshott CA, Parker GJ, Symms MR, Hickman SJ, Tofts PS, Miller DH, Barker GJ. ADC mapping of the human optic nerve: increased resolution, coverage, and reliability with CSF-suppressed ZOOM-EPI. *Magn Reson Med* 2002;47(1):24–31
- 13 Sherbondy AJ, Dougherty RF, Napel S, Wandell BA. Identifying the human optic radiation using diffusion imaging and fiber tractography. *J Vis* 2008;8(10):12.1–11
- 14 Yamada M, Momoshima S, Masutani Y, Fujiyoshi K, Abe O, Nakamura M, Aoki S, Tamaoki N, Okano H. Diffusion-tensor neuronal fiber tractography and manganese-enhanced MR imaging of primate visual pathway in the common marmoset: preliminary results. *Radiology*2008;249(3):855–864
- 15 Roebroek A, Galuske R, Formisano E, Chiry O, Bratzke H. High-resolution diffusion tensor imaging and tractography of the human optic chiasm at 9.4 T. *Neuroimage*2008;39(1):157–168
- 16 Hui ES, Fu QL, So KF, Wu EX. Diffusion tensor MR study of optic nerve degeneration in glaucoma. *Conf Proc IEEE Eng Med Biol Soc*2007; 2007:4312–4315
- 17 Song SK, Sun SW, Ramsbottom MJ, Chang C, Russell J, Cross AH. Demyelination revealed through MRI as increased radial (but unchanged axial) diffusion of water. *Neuroimage*2002;17(3):1429–1436
- 18 Tropine A, Vucurevic G, Delani P, Boor S, Hopf N, Bohl J, Stoeter P. Contribution of diffusion tensor imaging to delineation of gliomas and glioblastomas. *J Magn Reson Imaging*2004;20(6):905–912
- 19 Byrnes TJ, Barrick TR, Bell BA, Clark CA. Diffusion tensor imaging discriminates between glioblastoma and cerebral metastases *in vivo* *NMR Biomed*2011;24(1):54–60
- 20 Nickerson JP, Salmela MB, Koski CJ, Andrews T, Filippi CG. Diffusion tensor imaging of the pediatric optic nerve: intrinsic and extrinsic pathology compared to normal controls. *J Magn Reson Imaging*2010;32(1): 76–81
- 21 Wan SH, Xiao XL, Zhang XL. Comparative study of MRI and diffusion tensor imaging in acute optic neuritis. *Zhonghua Fangshexue Zazhi*2009; 43(2):166–169